

# Reduced Critical Current Spread in Planar MgB<sub>2</sub> Josephson Junction Array Made by Focused Helium Ion Beam

L. Kasaei, *Student Member, IEEE*, T. Melbourne, M. Li, V. Manichev, F. Qin, H. Hijazi, L. C. Feldman, T. Gustafsson, B. A. Davidson, X.X. Xi, and Ke Chen

**Abstract**— We have fabricated series arrays of closely spaced planar Josephson junctions on MgB<sub>2</sub> films using a 30 keV focused helium ion beam. Uniformity of junction parameters within the arrays was sufficient for achieving phase-lock into an applied microwave signal and flat giant Shapiro steps were observed. The spread in critical current of a 60-Josephson junction array (JJA) was estimated to be less than 3.5%, significantly better than reported in MgB<sub>2</sub> junctions fabricated by other techniques. These results demonstrate the potential of the focused He<sup>+</sup> ion beam irradiation technique in MgB<sub>2</sub> Josephson multi-junction circuit applications such as quantum voltage standards.

**Index Terms**— Focused helium ion microscope (HIM), Josephson junction and series array, lumped array, MgB<sub>2</sub>, voltage metrology.

## I. INTRODUCTION

Josephson junctions (JJs) are the basic building blocks of superconducting electronics. A reliable and reproducible technique to fabricate junctions is necessary for scaling up superconducting circuits. One application of the Josephson effect is in electrical metrology. A conventional Josephson Voltage Standard (JVS) has been a better alternative to a Weston cell with improved accuracy of dc voltage measurement. The primary reason is that the Josephson voltage depends only on the frequency which can be obtained from atomic clock (known with better than  $1.7 \times 10^{-16}$  uncertainty) [1]. Currently, the programmable Josephson voltage standard (PJVS) is widely used for dc and ac voltage calibration [2]. The pulse-driven ac Josephson voltage standard (ACJVS) is used for audio frequency applications and low voltage applications as quantum voltage noise source (QVNS) for noise thermometry [3]. These devices all require series arrays consisting of thousands of identical JJs with sufficiently low parameter spreads

This material is based upon work supported by the National Science Foundation under Grant No. DMR-1310087.

(Corresponding author: Leila Kasaei.)

Authors L. Kasaei, T. Melbourne, F. Qin, B. A. Davidson, X. X. Xi, and Ke Chen are with the Physics Department, Temple University, Philadelphia, PA 19122, USA, e-mail: [leila.kasaei@temple.edu](mailto:leila.kasaei@temple.edu).

Authors M. Li, V. Manichev are with department of Chemistry and Chemical Biology, Rutgers University, Piscataway, 08854, NJ, USA

Authors L. C. Feldman, T. Gustafsson, and H. Hijazi are with department of Physics and Astronomy, Rutgers University, Piscataway, NJ, 08854, USA

Color versions of all of the figures in this paper are available online at <http://ieeexplore.ieee.org>.

of the junctions, i.e. critical current and normal resistance. It is also beneficial to develop lumped-element arrays instead of distributed arrays. In a lumped-element array, all of the junctions are placed in less than one-quarter of the wavelength of the RF drive frequency so that the phase of the junctions is synchronized by the applied RF signal leading to a higher voltage for a given microwave. This sets a stringent limit for the spacing between adjacent junctions in the array. For instance, a drive frequency of 16 GHz and 13500 series junctions requires a 120 nm spacing [4]. Moreover, heat generated in the stacked JJ array is difficult to be dissipated compared to a planar configuration, which allows the heat to be readily transferred to the substrate [5]. The quality of the Nb-based JJ array is excellent, fabrication of 1000 Nb/Al-AIO<sub>x</sub>/Nb JJs for very large scale integration (VLSI) have been reported with the  $I_c$  spread from 0.8% to 8% for JJs with sizes from 1500 nm down to 200 nm [6]. Besides, the  $I_c$  spread of less than 1.6% was obtained for a series array of 200 NbTiN/Al-AIN<sub>x</sub>/NbTiN Josephson tunnel junctions [7]. However, the transition temperature of Nb at 9.25 K or NbTiN at 14.2 K requires the device to operate at 4.2 K or < 10 K. Magnesium diboride (MgB<sub>2</sub>), a simple binary compound with a critical temperature ~ 40 K, superconducting energy gaps greater than 2 meV, and a relatively long coherence length (~ 5 nm) has attracted considerable interest as an alternative to Nb-based devices that can operate at ~20 K, where cheaper, more efficient and reliable cryocooling technology is available.

Besides specific applications, junction series arrays are a useful tool for measuring the parameter spread of Josephson junctions. The current state of the art Nb junction technology contains over 65,000 junctions [8, 9], impossible to measure individually to determine the junction parameter spread. The parameter spread obtained from measuring series arrays permits a quick evaluation, which can facilitate further improvement of junction production.

Ion-damaged planar junctions have been used as a promising approach in manufacturing superconducting circuits. Neon ion beam irradiated arrays of junctions have been reported on YBCO [10] and MgB<sub>2</sub> [11]. There are also reports on using oxygen ions to produce arrays [12], superconducting quantum interference devices (SQUIDS) [13], and Superconducting Interference Filters (SQIFs) [14] on YBCO. In recent years, focused helium ion beam irradiation attracted a lot of attention. He<sup>+</sup> ion microscope (HIM) is based on a gas-field ion source

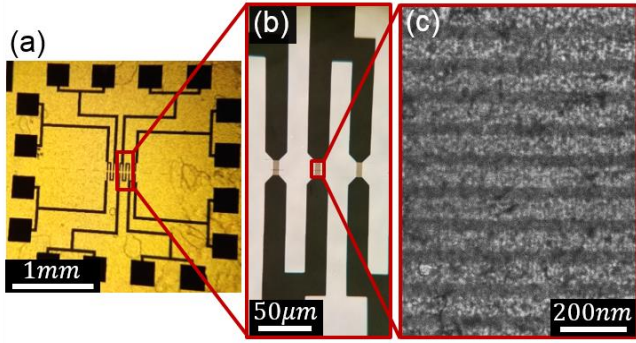


Fig. 1. (a) Optical image of the array pattern. Large bonding pads attached to a centered meandering micro-strips. (b) Three branches of the meander are enlarged. Dark color lines are Au covered MgB<sub>2</sub>. The tapered down bridges are SiO<sub>2</sub> covered MgB<sub>2</sub>. (c) Zoomed view of single tracks of He<sup>+</sup> irradiation at 100 nm inter-spacing on a 5 × 15 μm<sup>2</sup> bridge imaged in HIM.

(GFIS) with an ultra-sharp tip enabling the emission of an energetic beam stream of the gas ions with the diameter of less than 0.5 nm. The beam can introduce disorders into the superconducting film and suppress the critical temperature of the irradiated part, forming a barrier for a Josephson junction. This method has been well established and successfully implemented to fabricate YBCO [15, 16] and MgB<sub>2</sub> [17] Josephson junctions.

In this paper, we present the results of series arrays of planar MgB<sub>2</sub> Josephson junctions fabricated by the focused helium ion beam. With inter-junction spacing of 100 nm, a 60-JJ array showed the spread of critical current less than 3.5%, with operating temperature up to 28 K. The result is a substantial improvement in the parameter spread in MgB<sub>2</sub> Josephson junctions fabricated by all techniques.

## II. EXPERIMENTAL

Single JJ and series JJ arrays were fabricated using 25 nm thick MgB<sub>2</sub> thin films grown by hybrid physical-chemical deposition (HPCVD) on SiC substrates [18]. To protect the surface of the MgB<sub>2</sub> thin film from degradation during fabrication, a bilayer of Cr/Au (5 nm/20 nm) was deposited by DC magnetron sputtering on top of the film. 15 μm × 5 μm bridges and electrical bonding pads connecting to them were patterned by standard UV lithography and argon ion milling (see Fig. 1). A second lithography and ion milling were carried out to remove the Cr/Au bilayer on top of the bridges. A 4 nm SiO<sub>2</sub> thin film was then deposited on the entire sample by RF magnetron sputtering for protection against moisture. The sample was then loaded *ex-situ* into the chamber of a Zeiss Orion plus helium ion microscope. A single pixel line of 30 keV beam (the highest energy commonly available with the system with nominal beam diameter < 0.5 nm and pitch = 1 nm) was used to directly write Josephson junctions into the

plane of the thin film at room temperature. TRIM (Transport of ions in matter) software program [19] was used to simulate the He<sup>+</sup> ion beam interaction with the target material. The total thickness of the MgB<sub>2</sub> + SiO<sub>2</sub> protection layer (25+ 4 nm) was chosen to be substantially smaller than the projected range (PR) of the 30 keV He<sup>+</sup> ions in the target (> 150 nm). In fig. 2(a), damage density (displacement per volume, color scale) is shown within the sample suggesting that at displacement level ~ 1 × 10<sup>20</sup>/cm<sup>3</sup>, the width of the damaged region, is ~ 7.5 nm at the MgB<sub>2</sub>/SiC interface and ~ 1 nm at SiO<sub>2</sub>/MgB<sub>2</sub> interface. This lateral spread allows for observing the Josephson effect in the MgB<sub>2</sub> planar junctions. Fig. 2(b) shows the damage profile for top and bottom interfaces of MgB<sub>2</sub> film, indicating that the lateral spread of the damage characterized by the full width at half maximum (FWHM) is about doubled by the time ions reach the bottom of the film.

Our previous study on the irradiation effects in MgB<sub>2</sub> showed that increasing focused He<sup>+</sup> ion beam irradiation, induces gradual increase in resistivity and a gradual decrease in critical temperature of the damaged region [20]. When a dose of 8 × 10<sup>15</sup> ions/cm<sup>2</sup> is delivered to a large area, the material becomes normal at *T* > 4 K and dose of 2 × 10<sup>16</sup> ions/cm<sup>2</sup> produces a barrier for Josephson coupling across the damaged region [17].

Single JJs and nine series arrays with various number (10, 30, 50, 60) of JJs were written on different bridges using single pixel lines of He<sup>+</sup> beam with a dose of 2.7 × 10<sup>16</sup> ions/cm<sup>2</sup> and 100 nm inter-junction spacing (Fig. 1(c)). Here we discuss the results on 50- and 60-JJ arrays typical of the whole series. We also present the result of a single JJ for the comparison purposes.

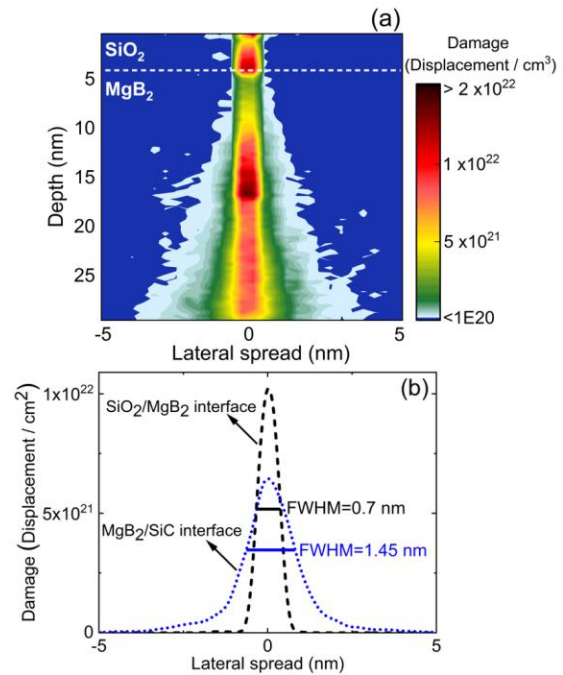


Fig. 2. (a) TRIM simulation of damage density in SiO<sub>2</sub>/MgB<sub>2</sub> (4+25 nm) film deposited on SiC substrate when irradiated with 2.7 × 10<sup>16</sup> ions/cm<sup>2</sup> He<sup>+</sup> ions. (b) Black dashed line represents damage profile at SiO<sub>2</sub>/MgB<sub>2</sub> interface. Blue dotted line represents damage profile at MgB<sub>2</sub>/SiC interface.

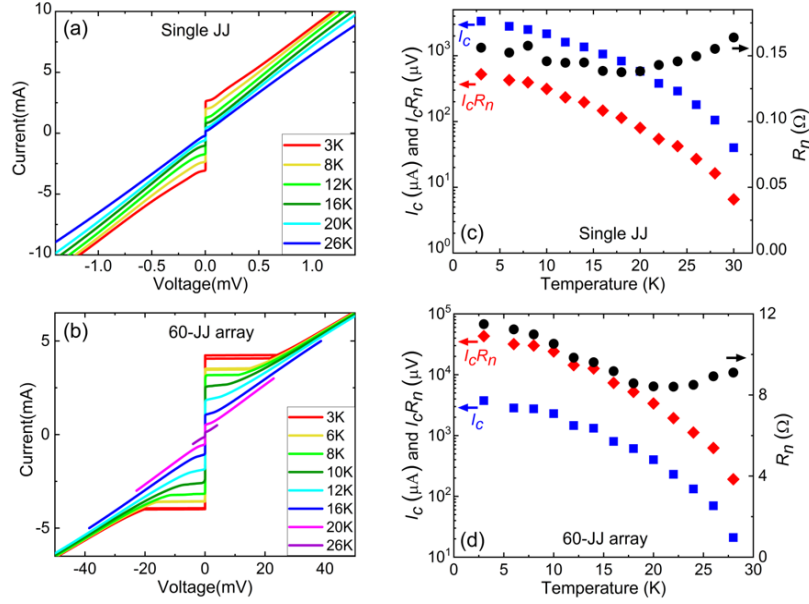


Fig. 3. Current-Voltage characteristics at different temperatures for (a) single JJ, (b) 60-JJ array. Temperature dependence of the junction normal resistance (black squares), critical current (blue circles) and critical voltage (red diamonds) for (c) single JJ, (d) 60-JJ array. Compared to the single junction, normal resistance of the arrays scales with the number of junctions in the array.

### III. RESULTS AND DISCUSSION

Fig. 3(a) and 3(b) show  $I$ - $V$  curves at different temperatures for the single JJ and the 60-JJ array, respectively. The fitted values of critical current ( $I_c$ ), normal resistance ( $R_n$ ), and characteristic voltage ( $I_c R_n$ ) to the resistively shunted junction (RSJ) model are plotted as a function of temperature in the Fig. 3(c) and 3(d). While the single JJ remained hysteresis-free down to the lowest measurement temperature of 3 K, the 60-JJ array became hysteretic at approximately 6 K. We barely observed any multiple steps around  $I_c$  of the array, which suggests minimal variations in the junction critical current in the array. For both the single JJ and the array data, the increase of resistance with increase in temperature and bias current indicates that the boundaries between the superconducting electrodes and the junction barrier move as temperature changes and the bias current varies, respectively, in agreement with the

previous ion-damaged junction study [21]. The shape of the hysteretic  $I$ - $V$  shown in Fig. 3(b) at low temperature is consistent with a SNS junction with high current density driven into non-equilibrium [22]. A couple of junctions could be hysteretic causing the hysteresis in a series array of Josephson junctions. There is a nearly constant critical current independent of the number of junctions ( $N$ ) and an almost linear increase of  $R_n$  with  $N$ ; subsequently the  $I_c R_n$  product also increases linearly with  $N$  (See table I.). While the normal resistance at 12 K for single JJ was 0.15  $\Omega$ , it rises to  $\sim 7.8 \Omega$  for the 50-JJ array and  $\sim 9.8 \Omega$  for the 60-JJ array, indicating good scaling with the single junction normal resistance. The value of  $I_c R_n$  product for the 60-JJ array at 12 K was  $\sim 14.4$  mV.

To verify that the arrays consist of Josephson junctions and assess their uniformity, the single JJ and arrays were exposed to RF radiation using an antenna placed above the chip.  $I$ - $V$  characteristics were observed while adjusting microwave power and frequency. Fig. 4(a) shows current-voltage characteristics of a single JJ with different applied microwave power at frequency 11.79 GHz, measured at 24 K. Fig. 4(b) and 4(c) show giant Shapiro steps in the  $I$ - $V$  curve of 50-JJ array and 60-JJ array when applying 11.76 GHz (at 24 K) and 12.35 GHz (at 24 K) RF radiation respectively. The Shapiro steps are expected to appear at voltages:  $V_n = Nn\Phi_0 f$ , where  $n$  is an integer representing the Shapiro step index and  $f$  is the frequency of the RF radiation, and  $\Phi_0$  is the flux quantum.  $N$  will be replaced by the number of JJs in the array or 1 in single JJ. The measurement of the first voltage step for single JJ ( $24.0 \mu\text{V} \pm 0.1 \mu\text{V}$ ), 50 JJA ( $1200 \mu\text{V} \pm 4 \mu\text{V}$ ), and 60 JJA ( $1500 \mu\text{V} \pm 4 \mu\text{V}$ ) agree with the expected voltages within the uncertainty of the measurement system. Consequently, it is evident

Table I. The dependence of  $R_n$  and  $I_c R_n$  on the number of junctions

Number of Junctions ( $N$ )	1	50	60
$R_n (\Omega)$ at 12 K	0.15	7.8	9.8
$\frac{R_n (\Omega)}{N}$	0.15	0.16	0.16
$I_c R_n$ (mV) at 12 K	0.23	13.3	14.4
$\frac{I_c R_n (\text{mV})}{N}$	0.23	0.26	0.24



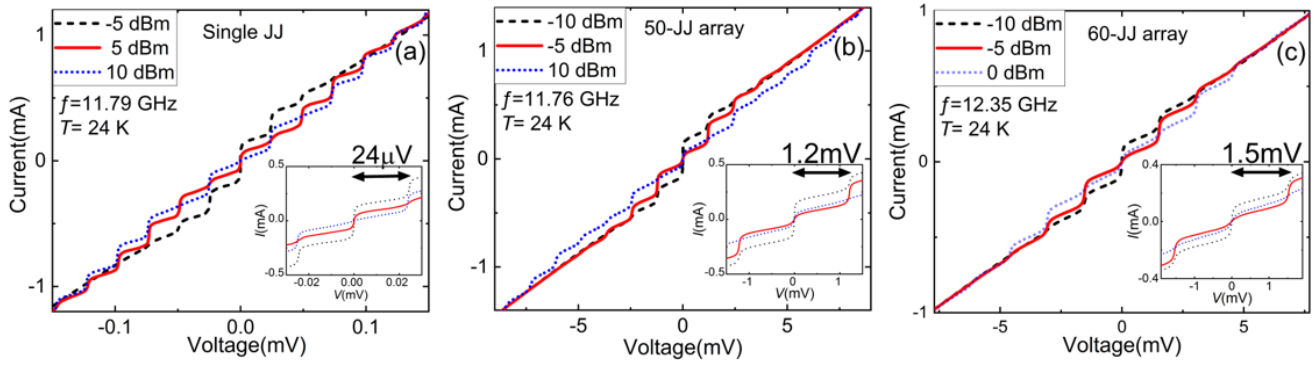


Fig. 4. (a) Current-Voltage characteristics for single junction at  $T = 24$  K under applied RF frequency of  $f = 11.79$  GHz. (b) Current-Voltage characteristics for 50-JJ series array at  $T = 24$  K under applied RF frequency of  $f = 11.76$  GHz. The space between adjacent steps in voltage is 50 times of that for an individual junction. (c) Current-Voltage characteristics for 60-JJ series array at  $T = 24$  K under applied RF frequency of  $f = 12.35$  GHz. The space between adjacent steps in voltage is 60 times of that for an individual junction.

that all the junctions are on the first step at the same time and that the junctions are tending to phase-locked to the RF current. The current amplitude of the 1<sup>st</sup> Shapiro steps (step width) in the arrays was about 0.15 mA. By reaching large step amplitude, the array would be less susceptible to noise-induced transitions between the quantized voltage states [3].

In order to examine the lateral homogeneity of the barriers, the critical current of the JJ is modulated by an applied magnetic field normal to the sample surface. In the case of a single JJ, a Fraunhofer pattern which is basically the modulus of the

Fourier transform of a constant critical current density within the junction is expected. In the planar geometry, the field inside the junction is much larger than the applied field due to the flux focusing effects [23] of the electrodes. Based on Rosenthal's result, we expect the first minima in Fraunhofer pattern occur at  $\sim \pm 0.15$  mT which agrees with the experimental result of  $\sim \pm 0.11$  mT as shown in Fig. 5(a). Fig. 5(b) and (c) illustrate the oscillatory behavior of critical current in the presence of magnetic field for 50- and 60-JJ arrays, respectively, which clearly deviates from a Fraunhofer pattern in that a plateau is formed at field around zero. The plateau suggests some magnetic field screening, possibly resulting from close inter-junction spacing of 100 nm, comparable to the London penetration depth of MgB<sub>2</sub> ( $\sim 100$  nm at the measurement temperature [24]), since no plateau and similar to single JJ Fraunhofer pattern was observed for a 10-JJ array with 1  $\mu$ m inter-junction spacing [25]. Further research is required to understand this phenomenon.

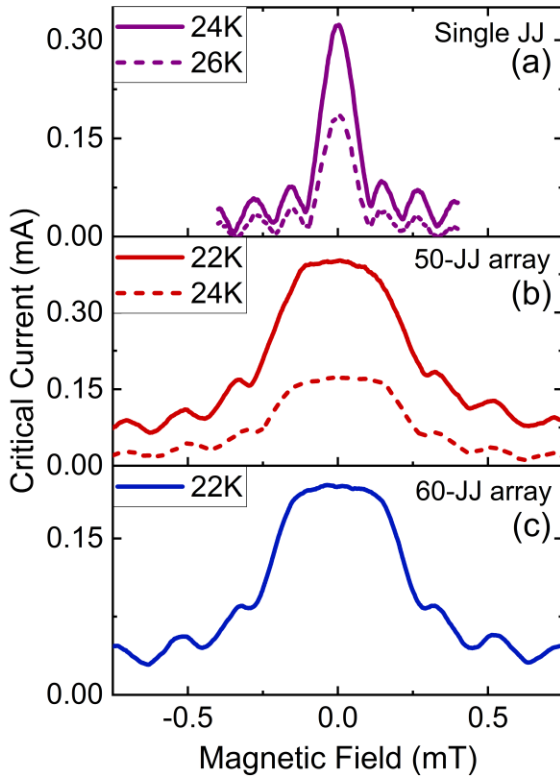


Fig. 5. Dependence of critical Josephson current on an applied magnetic field at different temperature for (a) single JJ, (b) 50-JJ array, (c) 60-JJ array.

Additional differential resistance calculations were performed at 12 K to reveal the distribution of the individual critical currents in 50- and 60-JJ array.  $I$ - $V$  curves exhibit RSJ-like behavior as low as 12 K while thermal smearing remains minimal. To evaluate the spread of the critical current in the 50- and 60-JJ arrays, we fit the experimental  $dV/dI$ - $I$  curves obtained by numerical differentiation of  $I$ - $V$  curves with calculated curves obtained by assuming a random Gaussian-type critical current distribution with a standard deviation  $\sigma$ , i.e., the  $I_c$  spread, in a series array consisting of JJs following the RSJ model at  $T = 0$ , namely  $V(I) = R_n \sqrt{I^2 - I_c^2}$  [26]. The normal resistance  $R_n$  was assumed to be constant for each junction to follow empirical observation. Thermal smearing effect is ignored to simplify calculations and will be analyzed separately. The fitting results in Fig. 6 show overall agreement between the experimental results and simple theoretical model except for double peaks in both 50- and 60-JJ array. The fitting parameter  $\sigma$  for the fitting is 4% and 3.5% for the 50- and 60-JJ arrays, respectively. Applying the same fitting method to a single JJ yields  $\sigma = 2\%$  which can be explained by thermal smearing that was ignored in the theoretical model. Subtracting the thermal smearing, from the given spreads for arrays would result in yet lower fabrication spread. The origin

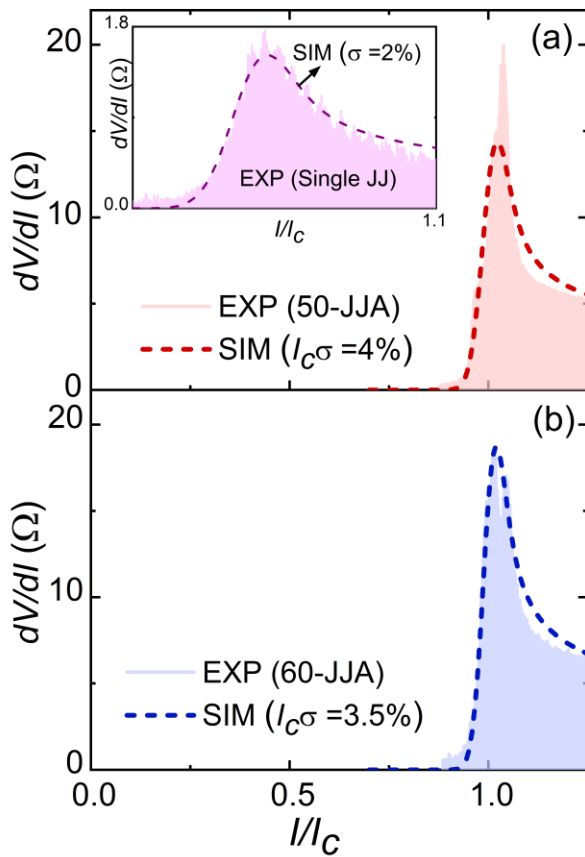


Fig. 6.  $dV/dI$  versus normalized current for (a) 50-, (b) 60-JJ array at  $T = 12$  K. The inset shows  $dV/dI$  versus normalized current for single junction. Dashed lines show the simulated curves with  $I_c$  spread  $\sigma = 4\%$  (50-JJ array) and  $\sigma = 3.5\%$  (60-JJ array). For single JJ, the fitting parameter is 2%. Note that the Simulated curves were generated by differentiating  $V(I) = R_n\sqrt{I^2 - I_c^2}$  at limiting case  $T = 0$  so the reported  $I_c$  spread for arrays can be considered an upper limit.

of the double peak in  $dV/dI$  curves is not determined yet. It should be noted that HIM was ran at reduced beam current, so to reach a certain dose ( $2.7 \times 10^{16}$  ions/cm<sup>2</sup>) the irradiation time was extended (up to  $\sim 20$  minutes for 60 JJA) which might have caused slight variation in the beam characteristic contributing to double peak features. To the best of our knowledge, the lowest reported value on the critical current spread was for a 100-JJ array of MgB<sub>2</sub>/MgO/MgB<sub>2</sub> tri-layer junctions showing 54% on-chip spread in critical current [27]. Our result corresponds to less than 3.5% spread for 60-JJ array indicating a homogeneous barrier over the larger length scale which is a significant improvement over prior attempts.

#### IV. CONCLUSION

In this paper we report the results of a series arrays of densely packed planar MgB<sub>2</sub> Josephson junctions fabricated by direct writing using a focused helium ion beam. The 60-JJ array showed excellent uniformity and reproducibility, with a spread of the array's critical currents being less than 3.5%, indicating excellent lateral homogeneity of the barrier. The normal resistance of the array scaled proportional to the num-

ber of junctions in the array. In addition,  $I_c$  modulation of arrays upon applying magnetic field, showed a plateau region at the center peak which needs further study. We speculate that dc SQUID magnetometers using closely spaced arrays in two arms can benefit from their properties of high  $I_cR_n$  product, high  $R_n$ , and less suppressed critical current under magnetic field, resulting in higher dynamic range, slew rate, and sensitivity than traditional dc SQUIDS formed by two single JJs. The results also pave the way for many other applications requiring tens to hundreds of MgB<sub>2</sub> Josephson junctions, such as voltage standard, quantum voltage noise source, and superconducting digital circuits, with operating temperatures above 20 K.

#### ACKNOWLEDGMENT

L. Kasaei acknowledges the use of services and facilities of Temple Materials Institute at Temple University.

#### REFERENCES

- [1] S. P. Benz, P. D. Dresselhaus, Y. Chong, and C. J. Burroughs, "Stacked nanoscale Josephson junction arrays for high-performance voltage standards," 2002.
- [2] H. Schulze, R. Behr, J. Kohlmann, F. Müller, and J. Niemeyer, "Design and fabrication of 10 V SINIS Josephson arrays for programmable voltage standards," *Superconductor Science and Technology*, vol. 13, no. 9, pp. 1293, 2000.
- [3] S. P. Benz, and C. A. Hamilton, "Application of the Josephson effect to voltage metrology," *Proceedings of the IEEE*, vol. 92, no. 10, pp. 1617-1629, 2004.
- [4] S. P. Benz, P. D. Dresselhaus, and C. J. Burroughs, "Nanotechnology for next generation Josephson voltage standards," *IEEE Transactions on Instrumentation and Measurement*, vol. 50, no. 6, pp. 1513-1518, 2001.
- [5] Y. Chong, P. D. Dresselhaus, and S. P. Benz, "Thermal transport in stacked superconductor-normal metal-superconductor Josephson junctions," *Applied physics letters*, vol. 83, no. 9, pp. 1794-1796, 2003.
- [6] S. K. Tolpygo, V. Bolkhovsky, T. J. Weir, L. M. Johnson, M. A. Gouker, and W. D. Oliver, "Fabrication process and properties of fully-planarized deep-submicron Nb/Al-AIO<sub>x</sub>/Nb Josephson junctions for VLSI circuits," *IEEE Trans. Appl. Supercond.*, vol. 25, no. 3, pp. 1101312, 2015.
- [7] H. Akaike, S. Sakamoto, K. Munemoto, and A. Fujimaki, "Fabrication of NbTiN/Al/AlN<sub>x</sub>/NbTiN Josephson junctions for superconducting circuits operating around 10 K," *IEEE Trans. Appl. Supercond.*, vol. 26, pp. 1100805, 2016.
- [8] S. Nagasawa, K. Hinode, T. Satoh, M. Hidaka, H. Akaike, A. Fujimaki, N. Yoshikawa, K. Takagi, and N. Takagi, "Nb 9-layer fabrication process for superconducting large-scale SFQ circuits and its process evaluation," *IEICE Transactions on Electronics*, vol. 97, no. 3, pp. 132-140, 2014.
- [9] Q. P. Herr, J. Osborne, M. J. Stoutimore, H. Hearne, R. Selig, J. Vogel, E. Min, V. V. Talanov, and A. Y. Herr, "Reproducible operating margins on a 72 800-device digital superconducting chip," *Superconductor Science and Technology*, vol. 28, no. 12, pp. 124003, 2015.
- [10] K. Chen, S. A. Cybart, and R. Dynes, "Study of closely spaced YBa<sub>2</sub>Cu<sub>3</sub>O<sub>7- $\delta$</sub>  Josephson junction pairs," *IEEE Transactions on applied superconductivity*, vol. 15, no. 2, pp. 149-152, 2005.
- [11] S. A. Cybart, K. Chen, Y. Cui, Q. Li, X. X. Xi, and R. Dynes, "Planar MgB<sub>2</sub> Josephson junctions and series arrays via nanolithography and ion damage," *Applied physics letters*, vol. 88, no. 1, pp. 012509, 2006.

- [12] A. Sharafiev, M. Malnou, C. Feuillet-Palma, C. Ulysse, T. Wolf, F. Couédo, P. Febvre, J. Lesueur, and N. Bergeal, "HTS Josephson junctions arrays for high-frequency mixing," *Superconductor Science and Technology*, vol. 31, no. 3, pp. 035003, 2018.
- [13] N. Bergeal, J. Lesueur, G. Faini, M. Aprili, and J. Contour, "High  $T_c$  superconducting quantum interference devices made by ion irradiation," *Applied physics letters*, vol. 89, no. 11, pp. 112515, 2006.
- [14] S. Ouanani, J. Kermorvant, C. Ulysse, M. Malnou, Y. Lemaître, B. Marcilhac, C. Feuillet-Palma, N. Bergeal, D. Créte, and J. Lesueur, "High- $T_c$  superconducting quantum interference filters (SQIFs) made by ion irradiation," *Superconductor science and technology*, vol. 29, no. 9, pp. 094002, 2016.
- [15] S. A. Cybart, E. Cho, T. Wong, B. H. Wehlin, M. K. Ma, C. Huynh, and R. Dynes, "Nano Josephson superconducting tunnel junctions in  $\text{YBa}_2\text{Cu}_3\text{O}_{7-\delta}$  directly patterned with a focused helium ion beam," *Nature nanotechnology*, vol. 10, no. 7, pp. 598, 2015.
- [16] E. Y. Cho, Y. W. Zhou, J. Y. Cho, and S. A. Cybart, "Superconducting nano Josephson junctions patterned with a focused helium ion beam," *Applied Physics Letters*, vol. 113, no. 2, pp. 022604, 2018.
- [17] L. Kasaei, T. Melbourne, V. Manichev, L. Feldman, T. Gustafsson, K. Chen, X. X. Xi, and B. Davidson, "MgB<sub>2</sub> Josephson junctions produced by focused helium ion beam irradiation," *AIP Advances*, vol. 8, no. 7, pp. 075020, 2018.
- [18] X. X. Xi, "MgB<sub>2</sub> thin films," *Superconductor Science and Technology*, vol. 22, no. 4, pp. 043001, 2009.
- [19] J. F. Ziegler, M. D. Ziegler, and J. P. Biersack, *SRIM: the stopping and range of ions in matter*: Cadence Design Systems, 2008.
- [20] L. Kasaei, M. Demir, P. Bhattarai, V. Manichev, M. Li, H. Hijazi, L. C. Feldman, T. Gustafsson, Y. Collantes, E. Hellstrom, X. X. Xi, K. Chen, and B. A. Davidson, "Normal-State and Superconducting Properties of Co-Doped BaFe<sub>2</sub>As<sub>2</sub> and MgB<sub>2</sub> Thin Films after Focused Helium Ion Beam Irradiation," To be published.
- [21] A. Katz, S. Woods, and R. Dynes, "Transport properties of high- $T_c$  planar Josephson junctions fabricated by nanolithography and ion implantation," *Journal of Applied Physics*, vol. 87, no. 6, pp. 2978-2983, 2000.
- [22] K. Likharev, "Superconducting weak links," *Reviews of Modern Physics*, vol. 51, no. 1, pp. 101, 1979.
- [23] P. A. Rosenthal, M. Beasley, K. Char, M. Colclough, and G. Zaharchuk, "Flux focusing effects in planar thin - film grain - boundary Josephson junctions," *Applied physics letters*, vol. 59, no. 26, pp. 3482-3484, 1991.
- [24] D. Cunnane, C. Zhuang, K. Chen, X. X. Xi, J. Yong, and T. Lemberger, "Penetration depth of MgB<sub>2</sub> measured using Josephson junctions and SQUIDs," *Applied Physics Letters*, vol. 102, no. 7, pp. 072603, 2013.
- [25] T. Melbourne, "Magnesium Diboride Devices and Applications," Temple University, 2018.
- [26] A. Barone, and G. Paterno, *Physics and applications of the Josephson effect*: Wiley, 1982.
- [27] T. Melbourne, D. Cunnane, E. Galan, X. X. Xi, and K. Chen, "Study of MgB<sub>2</sub> Josephson Junction Arrays and Sub- $\mu\text{m}$  Junctions," *IEEE Transactions on Applied Superconductivity*, vol. 25, no. 3, pp. 1-4, 2015.